Effect of dislocations on the Langer-Schwartz model of nucleation and growth

1992 J. Phys.: Condens. Matter 4 4359

(http://iopscience.iop.org/0953-8984/4/18/004)

J. Phys.: Condens. Matter 4 (1992) 4359–4371. Printed in the UK

Effect of dislocations on the Langer–Schwartz model of nucleation and growth

G Sundar and J J Hoyt
Department of Mechanical and Materials Engineering, Washington State University, Pullman, WA 99164, USA

Received 27 November 1991

Abstract. The Langer–Schwartz model of nucleation and growth has been extended to include the presence of dislocations. The increased nucleation rate of precipitates lying on dislocations, the growth rate of these ellipsoidal precipitates and the effects of heterogeneous site saturation have been included in the model. It is shown that the presence of dislocations can have a large effect on the overall phase separation kinetics at low initial supersaturations, but it is concluded that heterogenous nucleation cannot account for the observed discrepancies between the Langer–Schwartz theory and previously reported data on the Al–Zn system.

1. Introduction

The classical theory of nucleation, as elucidated by Gibbs [1] and Becker and Doring [2] predicts the rate of formation of stable embryos (droplets of an emerging phase) as a function of the degree of supersaturation in an initially homogeneous metastable system. For most systems, the nucleation rate predicted by the classical theory of nucleation varies from extremely low values to very large values through a narrow range of supersaturation, thus effectively defining the onset of nucleation. A number of experiments have been performed to measure this onset of nucleation and separation of phases in a supersaturated solution near its critical concentration. Unfortunately, most of the measurements have indicated dramatic differences between theory and experiment.

In 1962, Sundquist and Oriani [3] observed that in perfluoromethylcyclohexane plus methylcyclohexane liquid mixtures, the cloud point appeared at temperatures far below those predicted by the classical theory. This was confirmed by Heady and Cahn [4] who argued that the discrepancies observed by Sundquist and Oriani and themselves could not be explained by competing effects of heterogeneous nucleation. In 1974, Huang *et al* [5] tested the classical theory of nucleation of bubbles in liquid CO_2. They observed that CO_2 appeared 'supercooled' in the same liquid state at temperatures well below those predicted by the classical theory. The experiment was performed at constant density rather than the usual constant pressure, thus the supercooled liquid refers to the absence of vapour bubbles. Similar experiments on other binary mixtures (2-6-lutidine plus water [6], cyclohexane plus methanol [7] and isobutyric acid plus water [8]) near the critical point drew the same conclusions: the classical theory is not even approximately correct in predicting the onset of nucleation.

0953-8984/92/184359 + 13 $04.50

It was Binder and Stauffer [9] who first recognized that the source of discrepancies lay in the experiments which consisted of measurements of the cloud point, that is the temperature at which nucleation first becomes profuse. Cloud point measurements essentially determine the effects of both nucleation rate and growth rate of droplets. The nucleation of stable embryos and the growth of existing droplets both compete for the available supersaturated solute and, since the nucleation rate is a very strong function of supersaturation, the inclusion of a growth rate term in the kinetic theory can significantly affect the predicted number of droplets formed.

In the light of this, Binder and Stauffer argued that the experimentally meaningful quantity is not the nucleation rate alone but the time required for the supersaturation to go to zero, which implies that, in addition to the nucleation rate, the droplet growth too should be taken into consideration. Using these ideas, Langer and Schwartz (LS) [10] derived a set of coupled differential equations which describe the decrease with time of supersaturation and increase with time of the average droplet size in a homogeneous system. The LS results show that, for small initial supersaturation, the inclusion of the growth rate leads to a much longer completion time for the phase transition reaction than that predicted by the classical theory.

The kinetics of phase separation in solids are much slower and thus nucleation rate measurements can be made more accurately than in liquids. One can thus avoid cloud point determinations which are essentially studies of 'completion time'. It should be noted however that separately measuring nucleation and growth rates in solids is difficult in that the nuclei do not become detectable until they have grown to a sufficient size. The first attempt to study the nucleation phenomenon in solids was made by Servi and Turnbull [11]. They investigated homogeneous nucleation kinetics in FCC Cu-rich Cu–Co alloys using resistivity measurements. The same system was studied again in 1984 by LeGoues and Aaronson [12] who employed transmission electron microscopy. These studies showed agreement within an order of magnitude of the classical nucleation rate but did not attempt to measure changes in supersaturation as a function of time.

In 1984, Simon *et al* [13] performed nucleation experiments on dilute Al–Zn alloys and analysed the small-angle x-ray scattering data in terms of the LS model. Their results showed some discrepancies with the LS model, including one data point which seemed to confirm the classical theory without inclusion of the growth rate.

An important effect concerning nucleation and growth which arises when considering alloy systems and a possible explanation for the differences between the results of Simon *et al* and the LS prediction is the presence of heterogeneous nucleation sites such as dislocations. It is widely known that nucleation occurs preferentially on dislocations due to release of the elastic energy associated with the line defect and reduction of the total interfacial free energy required. A theoretical treatment of nucleation on dislocations has been presented by Cahn [14]. He assumed that the elastic energy of the dislocation enclosed in the volume of the embryo was released and predicted the existence of metastable cylindrical embryos surrounding all dislocations in supersaturated systems. Lyubov and Solovyev [14] extended Cahn's treatment for coherent nuclei and suggested that the catalytic effect of dislocations was due to the presence of solute atmospheres which reduced the amount of solute required by the second phase. Aaronson *et al* [16] clarified this point by explaining that the formation of Cottrell atmospheres is a consequence of the tendency to equilibrate the chemical potential of the solute atoms in the system and therefore the actual driving force energy for nucleation is not affected; it was further pointed out that the nucleation process occurs faster because of more rapid transport of the solute to the developing embryos. Dollins [17] presented a treatment for nuclei forming not on a dislocation line but on the surroundings.

Owing to this catalytic effect of dislocations, one would, therefore, expect the supersaturation to decrease more rapidly with time in the presence of dislocations than it would in a homogeneous system.

The purpose of this work is to extend the LS model to the case where nuclei are forming on both dislocations and the bulk material and examine the effects, if any, on the LS results of preferred nucleation at dislocations. In addition, the results of the present investigation will allow us to decide whether the discrepancies between the Al–Zn data of Simon *et al* and the LS model are due to the presence of dislocations.

In the extension of the LS model, a number of rather drastic and inelegant assumptions shall be made. Perhaps the most drastic one concerns the nature of the nucleus located at the dislocations and in the bulk. For a heterogeneous nucleation catalytic effect to take place, an incoherent particle must be assumed. An incoherent particle is one whose interface with the matrix has a different atomic configuration than that of either of the phases. Incoherent homogeneous nucleation, however, has not been observed in any alloy system. Nevertheless, in several alloy systems, such as Al–Zn, metastable coherent nucleation in the bulk competes with stable incoherent precipitation at heterogeneous sites. Thus, despite the above assumptions and subsequent simplifications, it is hoped that the model at least qualitatively describes real alloy systems.

2. The Langer–Schwartz model

The Langer–Schwartz (LS) model [10] is a statistical theory of nucleation and growth which describes the kinetics of unmixing of slightly supersaturated off-critical fluids. The four relevant quantities considered in the kinetics of nucleation and growth are supersaturation, droplet size, droplet density and time. Using concepts of scaling [18], LS introduced four reduced parameters. The first is the supersaturation

$$y(t) = x(t)/x_0 \tag{2.1}$$

where

$$x(t) = 2\delta C(t)/(\beta \Delta C) = (2/\beta)\,(C_m(t) - C_A)/(C_B - C_A). \tag{2.2}$$

The quantity $\beta \approx \frac{1}{3}$ is the power-law exponent of the miscibility gap, $C_m(t)$ is the solute concentration of the matrix at time t and C_A and C_B are the equilibrium concentrations of the matrix and the second phase respectively. The term x_0 appearing in equation (2.1) is defined as

$$x_0 = 4(\sigma\zeta^2/kT_c)^{1/2}$$

where ζ is the correlation length, σ the interfacial energy and T_c the critical temperature. The second scaled parameter defined by LS is the reduced time, which is given by

$$\tau = (Dx_0^3/24\zeta^2)t \tag{2.3}$$

with D the diffusion coefficient. The third and fourth scaled variables are the mean droplet radius ρ and the number density n which are given by

$$\rho = Rx_0/2\zeta \qquad n = 64\pi(\zeta/x_0)^3 N. \tag{2.4}$$

In equations (2.3) and (2.4), t, R and N are the real time, real size and real number density respectively.

The two differential equations which describe the time dependencies of all the relevant quantities in the phase separation reaction are

$$d\rho/d\tau + (\rho/3)(1/(y_1 - y) + \varphi/y(y\rho - 1))\, dy/d\tau = -\rho^4 J(y)/3x_0(y_1 - y) \tag{2.5}$$

$$d\rho/d\tau + (\varphi/y^2)\, dy/d\tau = (1/\rho^2)(y\rho - 1) + [\rho^3 J(y)/x_0(y_1 - y)](a - \rho + 1/y) \tag{2.6}$$

where a is a constant and y_1 is the initial value of the scaled supersaturation, $y_1 = y(\tau = 0)$.

The term φ is equal to zero for $R - R^* > \frac{1}{2}R^*$ and equal to a constant for $R - R < \frac{1}{2}R^*$. The numerical value of this constant is found by comparing the long-time coarsening behaviour of these equations to the Lifshitz–Slyozov theory [19].

The nucleation rate $J(y)$ appearing in equations (2.5) and (2.6) is given by

$$J(y) = Ay^{2/3}(1 + y)^{3.55} \exp(-1/y^2) \tag{2.7}$$

where $A \approx 3$. LS point out that, for most systems, x_0 will be of the order of unity and that the ratio $(x/x_0)^2$ (or $1/y^2$) is equal to the W^*/kT term found in classical nucleation theory. It is worth noting that all the temperature-dependent quantities have disappeared in equations (2.5) and (2.6); that is, one should be able to map the behaviour observed at one temperature on that at another simply by rescaling lengths and times according to equations (2.3) and (2.4).

3. Extension of the Langer–Schwartz model

It was mentioned in the Introduction that nucleation occurs preferentially on dislocations due to the release of elastic energy and the reduction of the total interfacial free energy required. Therefore, in addition to the second-phase particles growing homogeneously, the dislocation-nucleated particles too would contribute to the depletion of the surrounding supersaturated material. This contribution can be taken into account by simply adding a term in the conservation of solute condition given by LS as

$$(\delta C(t = 0) - \delta C(t))/(\Delta C - \delta C) \approx \tfrac{4}{3}\pi \bar{R}^3 N + Z_d.$$

Assuming that $\beta \approx \frac{1}{4}$, we have

$$x_1 - x = n\rho^3 + 6Z_d$$

for particles growing on the dislocations.

It is the purpose of this section to find an expression for Z_d and incorporate it in the LS equations. The three basic ingredients which go into the calculation of Z_d are the nucleation rate on dislocations, the growth rate of the dislocation-nucleated nodules and the impingement of these nodules on each other. Section 3.1 uses Cahn's treatment of nucleation on dislocations [14] to quantify the catalytic effect of the dislocations. An expression for nodule growth rate is derived in section 3.2 and in section 3.3 the volume fraction is evaluated after taking into account the mutual impingement of nodules. The final rate equations are presented in section 3.4.

The calculation of Z_d centres around the problem of impingement [20]. The LS model was based on the implicit assumption that the probability of any small region transforming in a given time interval will be the same in all parts of the untransformed volume. Since the model deals with low initial supersaturations, the probability of nodules impinging upon each other is very low. In the presence of dislocations, however,

the situation is more complex. Dislocations exhibit a relative ease of nucleation and can get saturated easily due to a relatively fewer number of nucleation sites. Impingement therefore becomes a very likely event in the present case.

The concept of extended line intercept [21] is used to calculate the total volume of nodules originating from a dislocation line, assuming impingement only with other nodules nucleated on the same dislocation line. A random distribution of dislocation lines is then considered in order to allow for impingement of regions nucleated on different dislocation lines. In addition, an anisotropic growth rate is assumed for the nodules growing on the dislocations whose shape stays constant.

3.1. Nucleation on dislocations

The first theoretical treatment of nucleation on dislocations was presented by Cahn [14] in 1957. He assumed that the nucleus lies along the dislocation and has a circular cross-section perpendicular to the dislocation line. The radius of the cross-section is not constant but varies with the distance along the line. In addition to the usual volume and surface-energy terms in the expression for the energy of formation of the nucleus of a given size, there is a term representing the strain energy of the dislocation in the region now occupied by the new phase. The work of formation per unit length of dislocation line is then

$$W_d = -A \log r + 2\pi\sigma r - \pi f r^2$$

where W_d is the free-energy change of formation of nucleus per unit length of dislocation, $A = Gb^2/4\pi(1-\nu)$ for edge dislocations and $Gb^2/4\pi$ for screw dislocations, G is the elastic shear modulus, b is the magnitude of Burgers vector, ν the Poisson ratio, σ the interfacial energy between the particle and the matrix and f the negative of the volume free energy of formation of the new phase.

The energy of the whole nucleus can be obtained by integrating the above expression along the effective length of the nucleus. To find the nucleation rate, the combination of size and shape which gives the saddle-point energy change for the whole nucleus is required. Cahn solved this problem by applying appropriate boundary conditions; the critical nucleus is defined in terms of a maximum radius r_1 and a measure of its effective length l. Cahn's results are expressed in terms of the ratio of the critical work of formation of a heterogeneous nucleus to the corresponding free energy of a homogeneous spherical nucleus of critical size versus a parameter α defined as

$$\alpha = 2Af/\pi\sigma^2$$

Typical values of A, f and σ correspond to α values between 0.5 and 0.7. We take $\alpha = 0.6$ and recover a value of 0.2 for the fraction W_d^*/W^* from Cahn's work. Therefore, the scaled nucleation rate per unit length becomes

$$J_d = A'(Dx_0^6/\zeta^5)y^{2/3}(1+y)^{3.55}\exp(-0.2/y^2)(2\zeta/x_0)^2(24\zeta^2/Dx_0^3) \tag{3.1}$$

where $A' = 1/288\pi\sqrt{3}$. In obtaining the enhanced nucleation rate on dislocations we have assumed the pre-exponential factor to be the same as that of the homogeneous nucleation rate. Although this simplification is incorrect, it is found that large changes in the pre-exponential factor will have little effect on the final results. Later on in the development we shall multiply the dislocation nucleation rate stated above by the dislocation density in order to account for the low concentration of nucleation sites.

3.2. Growth rate

R. Gomez-Ramirez and G. M. Pound [22] hypothesized that the nucleation barrier W_d^* is only slightly shape-dependent and therefore the critical shape can be approximated by that of the family with the lowest nucleation barrier. They found that an ellipsoidal critical nucleus gave reasonable results for the calculation of W_d^*. We use their hypothesis for the calculation of growth rate and assume an ellipsoidal nucleus with an aspect ratio $\eta \approx 1.3$ which is recovered from Cahn's work with $\alpha = 0.6$. This aspect ratio is assumed to remain constant throughout the growth process.

We assume a quasi-stationary chemical potential outside the growing particle so that

$$\nabla^2 \mu = 0. \tag{3.2}$$

Since the growing nodule is assumed to be elliptical in shape, we represent equation (3.2) in an ellipsoidal coordinate system and obtain the solution [23]

$$\mu(x, y, z) = \alpha A_\lambda x + \beta B_\lambda y + \gamma C_\lambda z + D \tag{3.3}$$

where

$$A_\lambda = [(1 - e^2)/e^3]\{\tfrac{1}{2} \ln[(1 + \acute{e})/(1 - \acute{e})] - \acute{e}\}$$

$$B_\lambda = C_\lambda = [(1 - e^2)/2e^3]\{\acute{e}/(1 - \acute{e}^2) - \tfrac{1}{2} \ln[(1 + \acute{e})/(1 - \acute{e})]\}$$

and

$$\acute{e} = [(\alpha^2 - \beta^2)/(\alpha^2 + \lambda)]^{1/2}.$$

Here λ is the positive root of

$$x^2/(a^2 + \lambda) + y^2/(b^2 + \lambda) + z^2/(b^2 + \lambda) = 1$$

and a, b and e are the semimajor axes, semiminor axes and the eccentricity of the ellipsoid respectively.

At regions remote from the nodule, λ tends to infinity and A_λ, B_λ and C_λ tend to zero. Therefore $\mu(x = \infty, y = \infty, z = \infty) = D = \mu(m)$, where $\mu(m)$ is the chemical potential of the matrix. Applying this as a boundary condition on equation (3.3), we have

$$\mu - \mu(\mathrm{m}) = \alpha A_\lambda x + \beta B_\lambda y + \gamma C_\lambda z. \tag{3.4}$$

At this point we will not attempt to evaluate each constant α, β and γ appearing in the above equation, but instead adopt the following simplifying procedure. We will state the boundary condition at one point on the surface of the nodule (namely $x = 0$, $y = b$, $z = 0$), obtain the flux of solute at this point by evaluating the derivative of the resulting concentration field, assume that the particle maintains a constant aspect ratio over all time and, finally, balance fluxes to obtain a growth rate.

According to the Gibbs–Thomson relation, the increase in chemical potential of solute at a curved surface is proportional to the sum of the reciprocals of the two principal radii, R_1 and R_2, at any point on the surface. From the definition of principal radii one obtains $R_1 = b$ and $R_2 = \eta^2 b$ for the ellipsoidal particle at the surface position $x = 0$, $y = b$, $z = 0$. Therefore, following Marder [24], the appropriate boundary condition becomes

$$\mu(0, b, 0) = \mu(y = \infty) + [\sigma(1 - C_\mathrm{A})/(\Delta C b)](1 + 1/\eta^2). \tag{3.5}$$

When evaluating the growth rate of a precipitate located on a dislocation line, a

complication arises in that the solute may be transported to the surface either from the bulk material or, more rapidly, along the dislocation core region. The two contributions to the growth rate and the resulting effect on the asymptotic mean-field coarsening behaviour have been discussed by Hoyt [25]. In the present work, the flux contribution from the dislocation core will be neglected. This assumption is reasonable in that we are ultimately interested in the supersaturation of the entire matrix and the supersaturation contained in the dislocation lines represents a small fraction of the total.

To obtain the growth rate the following equation is employed:

$$dV/dt = (SD/\Delta C)(dc/dy)_{y=b} \tag{3.6}$$

where V is the volume of the ellipsoid given by

$$V = = \tfrac{4}{3}\pi ab^2 = \tfrac{4}{3}\pi\eta b^3$$

and S is the surface area:

$$S = 2\pi b^2 + 2\pi(ab/e)\sin^{-1} e = 2\pi b^2[1 + (\eta/e)\sin^{-1} e].$$

In addition, to convert from the chemical potentials appearing in equation (3.5) to concentrations, the following approximations given by LS are used:

$$\delta\mu = (\partial\mu/\partial C_A)\delta c \qquad d_0 = \sigma/[(\Delta C)^2\,\partial\mu/\partial C_A]$$

where d_0 is the capillary length. The final result for the growth rate becomes

$$db/dt = (1.6D/b)[(\delta C/\Delta C) - (1.6d_0/b)]. \tag{3.7}$$

Perhaps the most serious assumption used in the above analysis is the mean-field boundary condition $\mu = \mu(\infty)$ at $x, y, z \to \infty$. The approximation is reasonable for widely separated particles, but as we shall see in the following section, the precipitates lying on dislocations are expected to be closely spaced, if not overlapping. Thus, use of the mean-field assumption is a bit inconsistent, but a more accurate mathematical description would be a difficult proposition. We anticipate that any errors in the growth rate derived above will not seriously affect the final results.

3.3. Volume fraction

As mentioned before, the derivation of the volume fraction centres around the problem of impingement. Although it is assumed in the LS model that the equilibrium volume fraction of precipitates is small, the number of heterogeneous dislocation sites is also very small. In addition, the number of heterogeneous sites decreases with time due to prior nucleation events and the growth of pre-existing nodules. This site saturation effect can be accounted for via an extension of the analysis first proposed by Avrami [20].

In deriving an expression for the volume fraction as a function of time, it will be convenient to use a device used by Cahn [21] called the extended line fraction Z_e. In evaluating Z_e it is assumed that new particles can be nucleated at sites already occupied by other precipitates and the nodules can grow unimpeded through other nodules. Thus Z_e can approach infinity whereas the actual line length cannot be greater than unity. The extended line fraction Z_e is the sum of all lengths of an imaginary line parallel to the dislocation which are intercepted by the nodules divided by the length of the line. If

these interceptions are randomly distributed on the line, then the actual line fraction is given by

$$Z = 1 - \exp(-Z_e).$$

If r is the distance between the assumed straight dislocation and the imaginary line, then the volume occupied by the nodules originating from a unit length of the dislocation is

$$V = \int_0^\infty 2\pi r Z \, dr.$$

Randomly distributing the dislocations in a unit volume will give us

$$Z_d = 1 - \exp(-LV) \tag{3.8}$$

where L is the dislocation density and Z_d the volume fraction.

We employ the same technique for calculating Z_d for an elliptical nodule with an aspect ratio η, semimajor axes a and semiminor axes b. If r is the distance between the dislocation and the imaginary line, then the length of line segment AB intersecting the nodule is:

$$AB = (2/\sqrt{1-e^2})\sqrt{b^2 - r^2}$$

where $e = 2.6$ for $\eta = 1.3$.

The point on the surface of the ellipsoid given by $x = 0, y = b, z = 0$ has an outward velocity given by equation (3.7). Therefore,

$$AB = \frac{2}{\sqrt{1-e^2}}\left[\left(\int_0^\tau \frac{db}{d\tau'} d\tau'\right)^2 - r^2\right]^{1/2}.$$

Following Cahn [21] we obtain, for the extended length fraction starting at a time between τ and $\tau + d\tau$, the expression

$$Z_e = \begin{cases} \dfrac{2}{\sqrt{1-e^2}} \displaystyle\int_0^\tau \left[\left(\int_0^{\tau'} \frac{db}{d\tau''} d\tau''\right)^2 - r^2\right]^{1/2} J_d \, d\tau' & \text{if } b(\tau) > r \\ 0 & \text{if } b(\tau) < r \end{cases}$$

On scaling with definitions given in equations (2.3) and (2.4), the above equations become

$$Z_e = 0.106 \int_0^\tau \left[\left(\int_0^{\tau'} \frac{1.6y\rho_d - 1.28}{\rho_d^2} d\tau''\right)^2 - r^2\right]^{1/2} J_d \, d\tau'$$

where

$$J_d = 3y^{2/3}(1+y)^{3.55} \exp(-0.2/y^2).$$

Assuming random distribution of dislocations, the total extended length fraction Z becomes

$$Z = 1 - \exp(-Z_e)$$

and

$$V = \int_0^{b(\tau)} 2\pi r Z \, dr \tag{3.9}$$

where V is the volume of the second phase growing per unit length of the dislocation and $b(\tau)$ is the size of the nodule in the direction of the semiminor axes at any time τ. If L is the dislocation density and d is the reduced dislocation density, then using the reduced parameter for length, see equation (2.4), we have

$$d = L(2\zeta/x_0)^2.$$

Substituting the above expressing in equation (3.8), we have

$$Z_d = 1 - \exp(-dV') \tag{3.10}$$

where V' is the scaled version of the expression for V.

We are now in a position to state the final rate equations for nucleation and growth in the presence of dislocations:

$$\left[\frac{\rho x_0}{3[x_0(y_1 - y) - 6Z_d]} + \frac{\varphi\rho^4}{3y\rho^3(y\rho - 1)}\right]\frac{dy}{d\tau} + \frac{d\rho}{d\tau} = \frac{-\rho^4[J + (6/\rho^3)\,dZ_d/d\tau]}{3[x_0(y_1 - y) - 6Z_d]} \tag{3.11}$$

$$(\varphi/y^2)\,dy/d\tau + d\rho/d\tau = (1/\rho^2)(y\rho - 1) + J\rho^3(a - \rho + 1/y)/[x_0(y_1 - y) - 6Z_d] \tag{3.12}$$

where $y_1 = x_1/x_0$. Equation (3.12) has a non-integrable singularity since at $\tau = 0$, $y = y_1$ and $Z_d = 0$. Therefore, in order to remove this singularity, we consider the only possible choice for ρ, which would be $\rho(\tau = 0) = a + 1/y_1$.

4. Results and discussion

Solutions to equations (3.11) and (3.12) were obtained by using a standard fourth-order Runge–Kutta forward integration technique. All calculations on equations (3.11) and (3.12) were performed with $a = 0.2$, $x_0 = 1.0$ and φ as defined elsewhere in the present work. Variations of y versus τ were plotted for different values of initial supersaturation y_1 ranging from extremely low values ($y_1 \approx 0.20$) to significantly large values ($y_1 \approx 0.50$). The effects of presence of dislocations on the nucleation and growth phenomenon were measured by plotting the same graphs for different dislocation densities.

In the computations we have attempted to use parameters consistent with the Al–Zn results of Simon *et al*. The reduced density parameter d is related to the real density L by the expression

$$d = L(2\zeta/x_0)^2.$$

The correlation length ζ as quoted by Simon *et al* [13] was of the order of 10^{-7} cm which yields a value of $d \approx 10^{-6}$ for $L \approx 10^8$ cm per cm^3. This value of L is typical for a well annealed alloy. The two values of d considered in the present study are $d = 5 \times 10^{-6}$ and $d = 5 \times 10^{-5}$ respectively.

Figure 1 shows the supersaturation as a function of time for an initial supersaturation of 0.2. At $y_1 = 0.2$, that is, initial activation energies of the order of 20 kT or greater, y remains essentially unchanged in the initial stages of nucleation and growth. Here, the nucleation rates, both on the dislocations and in the bulk, are too low to produce sufficient amounts of transformation products that could have any appreciable effect on the surrounding supersaturated material. The system continues to behave in this fashion

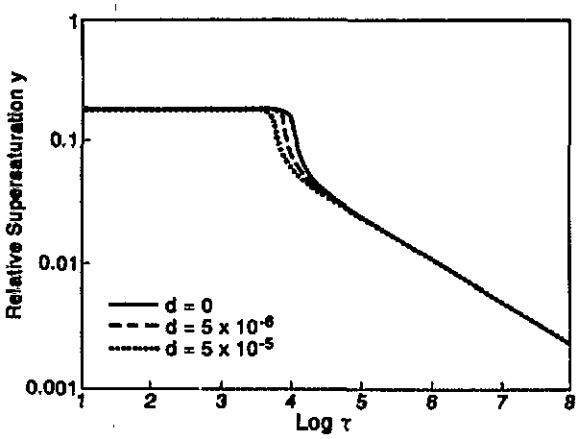

Figure 1. Computed relative supersaturation as a function of reduced time τ for $y_1 = 0.2$. Reduced dislocation densities are indicated in the insert.

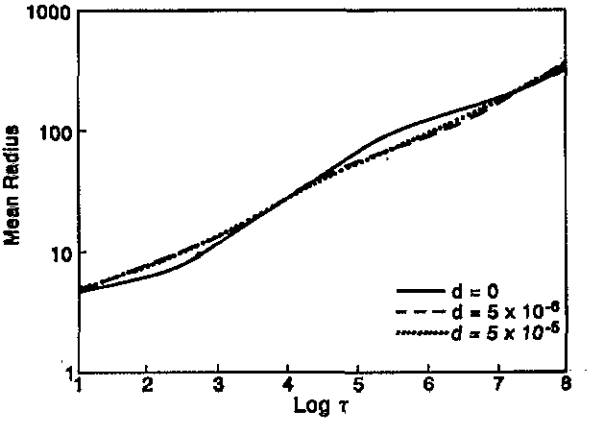

Figure 2. Scaled mean radius ρ as a function of time τ for $y_1 = 0.2$.

until a relatively small number of nodules become large enough to deplete the supersaturation significantly. The supersaturation y, therefore, undergoes a downward transient. For $y_1 \approx 0.2$, this decrease happens in the vicinity of $\tau = 10^4$ for the case $d = 0$. In the presence of dislocations, however, this onset takes place sooner owing to the effect of dislocation catalytic nucleation.

Figure 2 is a log–log plot of the dimensionless average radius ρ of the nodules growing in the bulk. For the LS case ($d = 0$), the particles undergo a period of free growth at early times. That is, the few nuclei present can acquire solute from the supersaturated matrix without competing with other particles. This mechanism of growth is reflected in the curve of figure 2 as a slope of ρ versus τ which is greater than $\frac{1}{3}$. At late times, when the particles compete with one another for the available solute, the Lifshitz–Slyozov $\tau^{1/3}$ result is seen. In the presence of dislocations, supersaturation diminishes at a faster rate due to the catalytic nucleation effect. As a result the period of free growth is greatly reduced.

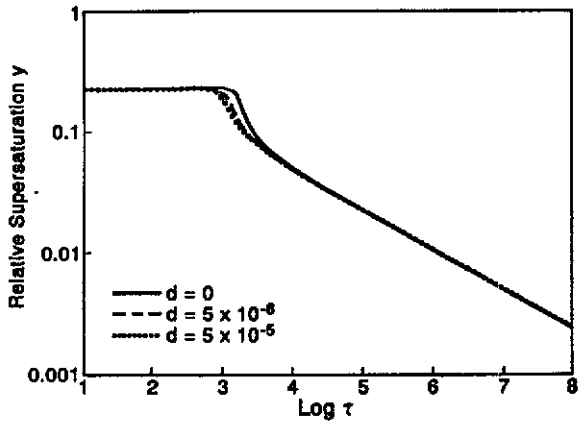

Figure 3. Computed relative supersaturation y as a function of time τ for the case $y_1 = 0.24$.

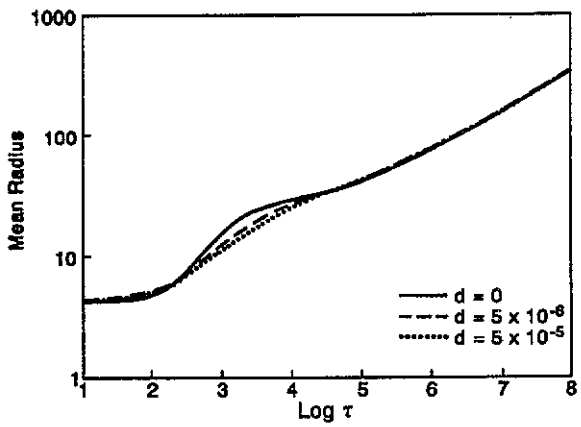

Figure 4. Scaled radius ρ as a function of time τ for the case $y_1 = 0.24$.

The kinetic behaviour for the average radius and the supersaturation at a somewhat higher initial supersaturation $y_1 = 0.24$ is shown in figures 3 and 4. The important point to note concerning the higher initial supersaturation is that although the supersaturation again decreases faster in the dislocation case, the effect is not as pronounced as in the $y_1 = 0.2$ case. The reason for the diminished dislocation effect at higher initial supersaturations is that the bulk nucleation rate increases faster with supersaturation than does the dislocation nucleation rate. In addition, even though dislocation nucleation has increased at $y_1 = 0.24$, the number of sites available has remained the same and the Avrami equation for Z_d comes into play.

A comparison of the effects of dislocations on the initial supersaturation is shown in figure 5, which is a log–log plot of the half-completion time $\tau_{1/2}$ (that is $y(\tau_{1/2}) = y_1/2$) versus y_1. It is evident that, at initial supersaturations of y_1 greater than 0.30, the presence of dislocations has practically no effect on the half-completion time $\tau_{1/2}$. Also shown in figure 5 are the data of Simon *et al* [13]. It can be seen that, although the presence of dislocations can have a large effect on the half-completion time at small values of y_1, it

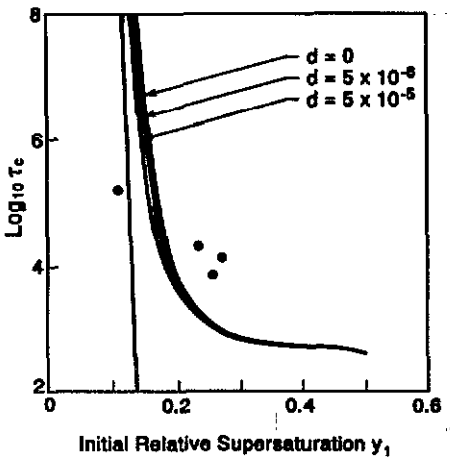

Figure 5. Half-completion time τ_c as a function of initial supersaturation y_1. The nearly vertical line is the classical nucleation time. Also shown are the Simon *et al* [13] data points for Al–Zn.

is doubtful that heterogeneous nucleation can explain the data point of Simon *et al* which is located nearly on the classical theory curve. Thus at this point it is unclear why the model and experiment disagree and therefore we are conducting further experiments on the Al–Zn system.

5. Conclusions

An extension of the Langer–Schwartz model of nucleation and growth has been developed which accounts for the presence of dislocations in an alloy system. The many assumptions made during the analysis suggest that the conclusions drawn will be qualitative. Nevertheless, it is clear that the overall phase separation kinetics are greatly enhanced in the presence of dislocations at low supersaturations. This is seen in terms of the decrease by nearly an order of magnitude in the half-completion time at reduced initial supersaturations of the order of 0.2. On the other hand, the kinetic behaviour is virtually unchanged for higher initial supersaturations.

In addition, it is unlikely that the discrepancy between the LS model and Al–Zn data reported by Simon *et al* can be attributed to heterogeneous nucleation events.

Acknowledgments

The authors would like to thank Professor John Hirth for a critical reading of the thesis on which this work is based. This work was supported by the National Science Foundation of the USA under contract number DMR-8919193. Finally, we wish to thank the reviewer of this paper for many helpful corrections.

References

[1] Gibbs J W 1948 *Collected Works* (New Haven, CT: Yale University Press) 1 105
[2] Becker R and Doring W 1935 *Ann. Phys.* **24** 719
[3] Sundquist B E and Oriani R A 1962 *J. Chem. Phys.* **36** 2604

[4] Heady R B and Cahn J W 1973 *J. Chem. Phys.* **58** 896
[5] Huang J S, Goldberg W I and Moldover M R 1975 *Phys. Rev. Lett.* **34** 639
[6] Schwartz A J, Krishnamurthy S and Goldburg W I 1980 *Phys. Rev.* A **21** 1331
[7] Huang J, Vernon S and Wong N C 1974 *Phys. Rev. Lett.* **33** 140
[8] Siebert E and Knobler C 1984 *Phys. Rev. Lett.* **18** 1133
[9] Binder K and Stauffer D 1976 *Adv. Phys.* **25** 343
[10] Langer J S and Schwartz A J 1980 *Phys. Rev.* A **21** 948
[11] Servi I S and Turnbull D 1966 *Acta Metall.* **14** 161
[12] Legoues F K and Aaronson H I 1984 *Acta Metall.* **32** 1855
[13] Simon J P, Guyot P and Ghilarducci de Salva A 1984 *Phil. Mag.* A **49** 151
[14] Cahn J W 1957 *Acta Metall.* **5** 169
[15] Lyubov B Y and Solovyev V A 1965 *Phys. Met.* **19** 13
[16] Aaronson H I, Kinsman K R and Rusell K C 1970 *Scr. Metall.* **4** 10
[17] Dollins C C 1970 *Acta Metall.* **18** 1209
[18] Stanley H E 1971 *Introduction to Phase Transitions and Critical Phenomenon* (New York: Oxford University Press)
[19] Lifshitz I and Slyozov V 1961 *J. Phys. Chem. Solids* **19** 35
[20] Avrami M 1939 *J. Chem. Phys.* **7** 1103
[21] Cahn J W 1956 *Acta Metall.* **4** 449
[22] Gomez-Ramirez R and Pound G M 1973 *Metall. Trans.* **4** 1563
[23] Carslaw and Jaeger 1986 *Conduction of Heat in Solids* 2nd edn (New York: New York Press)
[24] Marder M P 1986 *PhD Thesis* University of California, Santa Barbara
[25] Hoyt J J 1991 *Acta Metall. Mater.* **39** 209